Structural Engineering and Mechanics, Vol. 15, No. 5 (2003) 535-550
DOI: http://dx.doi.org/10.12989/sem.2003.15.5.535

A boundary radial point interpolation method (BRPIM) for 2-D structural analyses

Y. T. Gu† and G. R. Liu‡

Centre for Advanced Computations in Engineering Science (ACES),
Department of Mechanical Engineering, National University of Singapore,
10 Kent Ridge Crescent, Singapore 119260

(Received May 8, 2002, Accepted March 13, 2003)

Abstract. In this paper, a boundary-type meshfree method, the boundary radial point interpolation method (BRPIM), is presented for solving boundary value problems of two-dimensional solid mechanics. In the BRPIM, the boundary of a problem domain is represented by a set of properly scattered nodes. A technique is proposed to construct shape functions using radial functions as basis functions. The shape functions so formulated are proven to possess both delta function property and partitions of unity property. Boundary conditions can be easily implemented as in the conventional Boundary Element Method (BEM). The Boundary Integral Equation (BIE) for 2-D elastostatics is discretized using the radial basis point interpolation. Some important parameters on the performance of the BRPIM are investigated thoroughly. Validity and efficiency of the present BRPIM are demonstrated through a number of numerical examples.

Key words: meshless method; meshfree method; boundary integral equation; boundary element method; radial basis function; numerical analysis.

1. Introduction

Meshless or meshfree methods have attracted more and more attention from researchers in recent years, and are regarded as promising numerical methods for computational mechanics, as they do not require a mesh to discretize the problem domain, because the approximate solution is constructed entirely based on a set of scattered nodes. Several 'domain' type meshfree methods, such as Diffuse Element Method (DEM) (Nayroles *et al.* 1992), Element Free Galerkin (EFG) method (Belytschko *et al.* 1994), the method of finite spheres (De and Bathe 2000), Point Interpolation Method (PIM) (Liu and Gu 2001a), Local Point Interpolation Method (LPIM) (Liu and Gu 2001b), the Meshless Local Petrov-Galerkin (MLPG) method (Atluri and Zhu 1998), etc. have been proposed and achieved remarkable progress in solving a wide range of static and dynamic problems for solids and structures. Techniques of coupling meshfree methods with other established numerical methods have also been proposed, such as coupled EFG/FEM (Belytschko and Organ 1995, Hegen 1996), EFG/Boundary Element Method (BEM) (Gu and Liu 2001, Liu and Gu 2000). More detailed introductions of meshfree methods can be found in the monograph by Liu (2002).

† Ph.D.
‡ Professor

The Boundary Element Method (BEM) is a numerical technique based on Boundary Integral Equation (BIE), which has been developed since 1960's. For many problems, BEM is superior to the 'domain' type methods, such as Finite Element Method (FEM). BEM has a well-known dimensionality advantage for linear problems. For example, only 2-D bounding surface of a 3-D body needs to be discretized. However, in BEM, meshing is also a burdensome and expensive task for some problems, such as complicated boundary problems, 3-D problems and moving boundary problems.

Therefore, the idea of meshless has also been used for the BIE. The moving least squares (MLS) approximation is combined with BIE to propose a boundary type meshfree method called Boundary Node Method (BNM) (Mukherjee and Mukherjee 1997, Kothnur *et al*. 1999). The BNM has been applied to 3-dimesional problems in potential theory and elasto-statics (Chati and Mukherjee 2000, Chati and Mukherjee 1999). Very good results are obtained for these problems. However, because the shape functions based on the MLS approximation lack delta function property, it is difficult to satisfy the boundary condition in BNM efficiently. This problem becomes even more serious in the boundary type meshfree method because a large number of boundary conditions needs be satisfied. The method used in BNM to impose boundary conditions doubles the number of system equations, making BNM computationally much more expensive than the conventional BEM.

Scattered data interpolation by the radial basis function (RBF) began around 1960. The interpolation using radial basis function (RBF) is stable and flexible. In recent years, many researchers noticed its unique advantages, and used it to solve partial differential equations (Kansa 1990, Franke and Schaback 1997, Sharan *et al.* 1997). In the domain type meshfree methods, Liu *et al*. (Liu and Gu 2001c, Liu *et al.* 2002, Wang and Liu 2002) have been applied RBF for creating shape functions, which leads to the development of the radial point interpolation method (RPIM). A boundary type meshfree method, boundary radial point interpolation method (BRPIM), is proposed in this paper. In the BRPIM, the boundary of a problem domain is discretized by properly scattered nodes. The point interpolation using radial basis functions is utilized to construct shape functions with delta function properties. A proof is also given to show the partitions of unity property of the shape functions of the radial basis point interpolation. The BIE for 2-D elastostatics is discretized using this radial basis point interpolation. Because the shape functions possess delta function property, the BRPIM overcomes the shortcomings of BNM. The imposition of boundary conditions in the BRPIM is as easy as in the traditional BEM. The BRPIM has the same number of system equations as the conventional BEM. In addition, the rigid body movement can also be utilized to avoid some singular integrals. These advantages will be very beneficial to extend the present BRPIM to solve 3-D problems.

In this paper, the BRPIM is used for 2-D elastostatics. Several numerical examples are presented to demonstrate validity and efficiency of the BRPIM. A comparison study is carried out using the BRPIM, BNM, conventional BEM and analytical methods. The effects of some important parameters on the performance of the BRPIM are also investigated thoroughly, and the results are presented in detail.

2. Radial basis point interpolation

2.1 Shape functions of radial basis point interpolation

The point interpolants in the BRPIM are constructed on the 1-D bounding curve Γ of 2-D domain Ω, using a set of discrete nodes on Γ. As in the conventional BEM formulation, the displacement

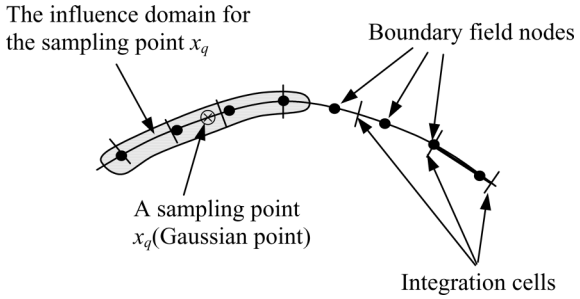

Fig. 1(a) The integration cells and influence domains used in the BRPIM

and traction can be constructed independently using point interpolation. The point interpolation for displacement $u(r)$ and traction $t(r)$ at a interpolation point (or a sampling point) r on the boundary Γ from the surrounding field nodes uses radial basis function can be written as

$$u=\sum_{i=1}^{n} b_i(r)\alpha_i=\boldsymbol{b}(r)\boldsymbol{\alpha} \tag{1a}$$

$$t=\sum_{i=1}^{n} b_i(r)\beta_i=\boldsymbol{b}(r)\boldsymbol{\beta} \tag{1b}$$

where r is a curvilinear distance (the arc length for 1-D curve boundary) on Γ, n is the number of field nodes (used to do the interpolation) in the influence domain (see Fig. 1a) of this point r, $b_i(r)$ is a radial basis function (RBF). α_i and β_i are the interpolation coefficients. In vector form, we have

$$\alpha^T=[\alpha_1, \alpha_2, \alpha_3, \ldots, \alpha_n] \tag{2a}$$

$$\beta^T=[\beta_1, \beta_2, \beta_3, \ldots, \beta_n] \tag{2b}$$

There are a number of radial basis functions (RBF), such as the multi-quadrics (MQ) radial function and Gaussian radial function. Characteristics of radial functions have been widely investigated (Kansa 1990, Franke and Schaback 1997). The variable in RBF is only the distance. Hence, the forms of interpolation formulations are the same for both 2-D problems and 3-D problems. The following multi-quadrics (MQ) radial function is used in this paper (other RBF can also used similar).

$$b_i(r)=(r_i^2+C^2)^q \tag{3}$$

There are two parameters, q and C, that need be determined in MQ radial function. q and C usually satisfy

$$q=I/2, \quad C>0 \tag{4}$$

where I is an odd integer. These two parameters will affect the performance of the MQ BRPIM.

However, there are still no successful rigorous methods to get theoretical best values for these parameters. In general, these two parameters can be determined by numerical examination. Detailed investigations of these parameters will be given for the present BRPIM in the following numerical examples.

The coefficients α_i and β_i in Eq. (1) can be determined by enforcing Eq. (1) to be satisfied at these n nodes in the influence domain of the interpolation point r. Eq. (1) can be then written in the following matrix form.

$$\boldsymbol{u}_n = \boldsymbol{B}\alpha \tag{5a}$$

$$\boldsymbol{t}_n = \boldsymbol{B}\beta \tag{5b}$$

where $\boldsymbol{u}_n$ and $\boldsymbol{t}_n$ are the vectors of nodal displacement and traction, given by

$$\boldsymbol{u}_n = [u_1, u_2, u_3, \ldots, u_n]^T \tag{6a}$$

$$\boldsymbol{t}_n = [t_1, t_2, t_3, \ldots, t_n]^T \tag{6b}$$

and $\boldsymbol{B}$ is a matrix of

$$\boldsymbol{B}^T = [\boldsymbol{b}_1(r_1), \boldsymbol{b}_2(r_2), \boldsymbol{b}_3(r_3), \ldots, \boldsymbol{b}_n(r_n)] \tag{6c}$$

Solving α and β from Eq. (5), and then substituting them into Eq. (1) leads to

$$u(r) = \Phi^T(r)\boldsymbol{u}_n \tag{7a}$$

$$t(r) = \Phi^T(r)\boldsymbol{t}_n \tag{7b}$$

where the shape function $\Phi(r)$ is defined by

$$\Phi^T(r) = \boldsymbol{b}^T(r)\boldsymbol{B}^{-1} = [\phi_1(r), \phi_2(r), \phi_3(r), \ldots, \phi_n(r)] \tag{8}$$

The matrix $\boldsymbol{B}$ is an $n \times n$ matrix. It needs to be invertible for the construction of the shape functions in Eq. (8). The existence of $\boldsymbol{B}^{-1}$ for arbitrary scattered nodes has been proven (Kansa 1990, Franke and Schaback 1997, Sharan *et al.* 1997). Therefore, in the BRPIM, the interpolation using radial basis function is stable and flexible. This advantage will be very beneficial to extend the present BRPIM to solve 3-D problems, in which the interpolation will be performed in a surface of the 3-D domain.

2.2 Properties of RPIM shape functions

The shape function $\phi_i(s)$ obtained through above procedure satisfies (Kansa 1990, Liu 2002)

$$\phi_i(r = r_i) = 1 \quad i = 1, n \tag{9a}$$

$$\phi_j(r = r_i) = 0 \quad j \neq i \tag{9b}$$

Therefore, the constructed shape functions have delta function property, and the boundary conditions

can be imposed in the same way as in the traditional BEM.

Although there is no constant term explicitly shown in the RBF in Eq. (3), the radial basis point interpolation can also theoretically satisfy the partitions of unity condition:

$$\sum_{i=1}^{n} \phi_i = 1 \tag{9c}$$

This can be proven in the following. An arbitrary complex function that has arbitrary order continuity can be expressed by an infinite Taylor series expansion. For the MQ RBF in Eq. (3), the Taylor series expansion at the vicinity of $r_q = 0$ can be given in the form of

$$b(r) = b(0) + b'(0)r + \frac{b''(0)}{2!}r^2 + \ldots = C^{2q} + b'(0)r + \frac{b''(0)}{2!}r^2 + \ldots \tag{9d}$$

It is now clearly seen that there is a constant term in Eq. (9d) because of $C \neq 0$ in Eq. (3). The presence of this constant basis can exactly reproduce a constant field following the same argument given in Section 5.5.2 of the monograph by Liu (2002), which states that the point interpolation can produce whatever is included in the basis functions. Note that the condition for the exact reproduction is that all the RBFs used in the radial point interpolation have to be evaluated exactly, meaning the expansion in Eq. (9d) needs to have infinite terms. It can now state that an exactly evaluated RBF in Eq. (3) contains a constant term and can reproduce a constant field. Following the same argument given in Section 5.5.3 (item 3) of the monograph by Liu (2002), for a given constant filed (it has been proven that the radial basis point interpolation can reproduce the constant field at an arbitrary point *r*), we have

$$u(r) = c = \sum_{i=1}^{n} \phi_i u_i = c \cdot \sum_{i=1}^{n} \phi_i \Rightarrow \sum_{i=1}^{n} \phi_i = 1 \tag{9e}$$

This shows that Eq. (9c) can be satisfied by the point interpolation using the RBF in Eq. (3).

In fact, the partition of unity property of the radial point interpolation can be understood intuitively. If the basis functions are smooth functions (to arbitrary order), these basis functions can then always be expanded in a Taylor series form. When $b(0) \neq 0$, there is always a constant term in the expanded basis functions. The reproductions of the point interpolation will always ensure the constant field to be produced (Liu 2002). The above proof is valid for all functions who satisfy the following two conditions: smooth to arbitrary order and $b(0) \neq 0$.

However, Eq. (9c) may not be satisfied exactly in the numerical tests. It is because there are always numerical errors in the computation of a complex RBF caused by the use of finite terms in the Taylor series. To demonstrate, a numerical test is used. Fig. 1(b) shows 25 regularly distributed field nodes and 4 arbitrary chosen sampling points. Table 1 lists the summations of shape functions at these four sample points. It can be observed that the radial basis point interpolation satisfy the partitions of unity condition in very high accuracy. The small errors are caused by the errors in the numerical evaluation of the complex RBF.

Note that RBF in Eq. (3) will not be linear reproduction, meaning the radial basis point interpolation cannot reproduce a linear field function. This is because no linear terms (due to $b'(0) = 0$) are included in Eq. (9d). This could be one of the major reasons for the poor *h*-convergence in using MQ RBFs for field variable interpolations. Hence, the linear polynomial terms are sometimes added in the radial basis point interpolation (1) to ensure the linear reproduction. It

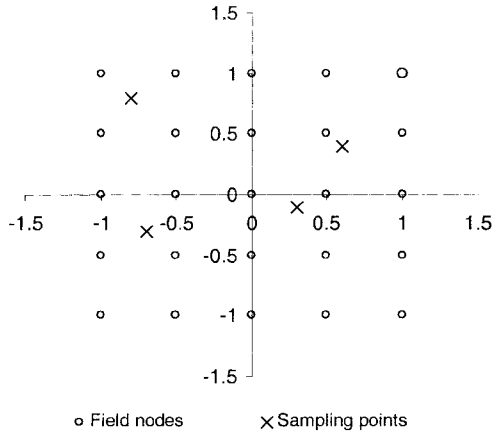

Fig. 1(b) 25 filed nodes and 4 sampling points for testing the partitions of unity property

Table 1 Results for testing the partitions of unity property of the radial basis* point interpolation shape functions in four sampling points

Coordinates of sampling points	$\sum_{i=1}^{25} \phi_i$
(−0.8, 0.8)	0.999935
(−0.7, −0.3)	0.999988
(0.3, −0.1)	1.0000574
(0.6, 0.4)	0.9999659

*C = 2.0, q = 0.5 in Eq. (3)

can also improve the accuracy for satisfaction of Eq. (9c) because the constant basis is included explicitly in the basis functions. However, the additional linear polynomial terms will increase the computational cost and it does not affect the computational accuracy very much for many practical problems (Liu 2002). Hence, the linear polynomial terms are not used in this study.

2.3 Influence domain

It can be found that the accuracy of interpolation depends on the field nodes used in the influence domain of a sampling point (the interpolation point). In the BRPIM, Gaussian quadrature is used to obtain the numerical integrations (discussed in the following section). In computation, Gaussian points (quadrature points) are taken as sampling points. Therefore, a suitable influence domain (as shown in Fig. 1a) should be chosen. In order to define the influence domain for a point r_i, a curvilinear influence domain is used. The arc length of the curvilinear domain d_{mi} is computed by

$$d_{mi} = \alpha_0 d_i \tag{10}$$

where α_0 is a scaling parameter, d_i is a parameter of distance (Liu 2002). If the nodes are uniformly distributed, d_i is the maximum distance between two nodes. In the case where the nodes are

randomly distributed, d_i can be defined as a characteristic arc length of the integration zone that contains point r_i (Belytschko *et al*. 1994). The integration zone is a background cell (as shown in Fig. 1a) for numerical integration. The number of nodes, n, can be determined by counting all the nodes in the influence domain. The parameter α_0 can be determined by numerical examination.

3. BRPIM formulation

3.1 Discrete equations of BRPIM

The well-known BIE formulation for 2-D linear elastostatics, presented by Brebbia (Brebbia 1978, Brebbia and Telles 1984), is given by

$$\boldsymbol{c}_i\boldsymbol{u}_i + \int_\Gamma \boldsymbol{u}\boldsymbol{t}^* d\Gamma = \int_\Gamma \boldsymbol{t}\boldsymbol{u}^* d\Gamma + \int_\Omega \boldsymbol{b}\boldsymbol{u}^* d\Omega \tag{11}$$

where c_i is a coefficient depended on the geometrical shape of boundary. $\boldsymbol{b}$ is the body force vector, $\boldsymbol{u}^*$ and $\boldsymbol{t}^*$ are the fundamental solution for linear elastostatics. The fundamental solution (Brebbia and Telles 1984) for 2-D plane strain problem is given by

$$u_{ij}^* = \frac{1}{8\pi G(1-\nu)}\left\{(3-4\nu)\ln\frac{1}{r}\delta_{ij} + r_{,i}r_{,j}\right\} \tag{12a}$$

$$t_{ij}^* = \frac{-1}{4\pi(1-\nu)r}\left\{\frac{\partial r}{\partial n}[(1-2\nu)\delta_{ij} + r_{,i}r_{,j}] - (1-2\nu)(r_{,i}n_{,j} - r_{,j}n_{,i})\right\} \tag{12b}$$

where G is the shear modulus, ν is the Poisson's ratio, δ is the Kronecker delta function, r is the distance between source point and field point, n is the normal to the boundary, a comma designates a partial derivative with respect to the indicated spatial variable.

Substituting Eq. (7) into Eq. (11) yields the BRPIM system equation

$$\boldsymbol{H}\boldsymbol{u}_n = \boldsymbol{G}\boldsymbol{t}_n + \boldsymbol{d} \tag{13}$$

where

$$\boldsymbol{H} = \boldsymbol{c}_i + \int_\Gamma \boldsymbol{t}^*\boldsymbol{\Phi}^T d\Gamma \tag{14a}$$

$$\boldsymbol{G} = \int_\Gamma \boldsymbol{u}^*\boldsymbol{\Phi}^T d\Gamma \tag{14b}$$

$$\boldsymbol{d} = \int_\Omega \boldsymbol{b}\boldsymbol{u}^* d\Omega \tag{14c}$$

There are two types of boundary conditions in the BRPIM

$$\boldsymbol{t} = \bar{\boldsymbol{t}} \qquad \text{on the natural boundary } \Gamma_t \tag{15a}$$

$$\boldsymbol{u} = \bar{\boldsymbol{u}} \qquad \text{on the essential boundary } \Gamma_u \tag{15b}$$

Because the shape functions of the BRPIM have delta function properties, the boundary conditions can be imposed in the same way as the traditional BEM. After applying the boundary condition, the system Eq. (13) has $2N_B$ equations and $2N_B$ unknowns for N_B boundary nodes. The system equation can be solved in a standard way to obtain the displacement and traction.

3.2 Comparison between BRPIM, BNM and BEM

BRPIM versus BEM

It can be found that the BRPIM and BEM are all based on the boundary integral equation. The difference is in the means of implementations.

The BRPIM uses radial basis functions, and BEM uses the polynomial basis functions. The number of basis function terms is the same as the number of field nodes used in interpolation. Therefore, the shape functions possess the delta function property and boundary conditions can be implemented with ease.

However, the BRPIM is a boundary type meshfree method when BEM is a boundary type method based on the predefined mesh. As other meshfree methods (e.g. EFG, BNM), the interpolation procedure in the BRPIM (Fig. 1a) is based only on a group of arbitrary distributed nodes as above discussed. The interpolation at a sampling point (Gaussian point) in the BRPIM is performed over the influence domain of this point, which may overlap with the influence domains of other sampling points. The interpolant procedure in BEM is based on an element. BEM defines the shape functions over predefined regions called elements, and there is no overlapping.

Compared with BEM, major disadvantages of the BRPIM are complexity of algorithm and some parameters that are needed to be defined by numerical examinations. In addition, the BRPIM is usually computationally more expensive than BEM because more interpolations nodes are used in the BRPIM.

BRPIM versus BNM

Both the BRPIM and BNM are boundary type meshfree methods. The difference between these two methods comes from the different interpolants utilized. As above discussed, the BRPIM uses radial basis point interpolation, in which the coefficients α and β in Eq. (1) are constant that are only determined by nodes selected in the influence domain. The Moving Least Squares (MLS) approximation is used in the BNM, in which α and β are also functions of curvilinear co-ordinate r. Therefore, the shape function of BNM is more complicated than that of the BRPIM. In addition, the shape function of BNM constructed using the MLS approximation lacks the delta function property. It takes extra effort to impose boundary conditions. The method used by Kothnur *et al.* (1999) to impose boundary conditions doubles the number of system equations ($4N_B$ equations for N_B boundary nodes and 2-D elasticity) making BNM computationally much more expensive than the conventional BEM.

3.3 Implementation of BRPIM

3.3.1 Singular integral

In order to obtain the integrals in Eq. (14), background integration cells that can be independent of the nodes are required. From Eq. (12), it is can be seen that the integrands in Eq. (14) consist of regular and singular functions. The regular functions in Eq. (14) can be evaluated using the usual

Gaussian quadrature based on the integration cells. In Eq. (14b), the matrix $\boldsymbol{G}$ contains a log singular integral. This type of singular integral can be evaluated by log Gaussian quadrature as follows:

$$I = \int_0^1 \ln(1/x) f(x) dx \cong \sum_{i=1}^{m} f(x_i) w_i \tag{16}$$

where the required points x_i and weights w_i are presented by Brebbia *et al.* (1984).

In matrix $\boldsymbol{H}$, $\boldsymbol{c}$ is a coefficient depended on the geometrical shape of the boundary, which is easy to be obtained for a smooth boundary. However, it is more complicated to obtain $\boldsymbol{c}$ for non-smooth boundaries. In addition, $\boldsymbol{H}$ contains $(1/r)$ type singular integral. Therefore, it can be a non-trivial task to directly evaluate the diagonal terms of $\boldsymbol{H}$. Note that shape functions of BRPIM possess delta function property and satisfy partitions of unity condition Eq. (9c), therefore, the rigid body movement can be utilized in this work to obtain the diagonal terms of $\boldsymbol{H}$ **(**Brebbia and Telles 1984).

3.3.2 Handling of corners with traction discontinuities

In handling traction discontinuities in corners, special care should be taken. Double nodes and discontinuous elements at corners are used to overcome this problem in the traditional BEM. Because there are no elements used in the BRPIM, a simple method proposed here to solve this difficulty is by displacing the nodes from the corner. In addition, the influence domain for interpolation is truncated at the corner. The method is very easy to implement and is used in the following numerical examples. The simple method is proven to be very accurate (Kothnur *et al.* 1999).

However, this technique does not work in general for boundary type meshfree methods for 3-D problems. To find an efficient method to handle traction discontinuities in boundary-type meshfree methods is still an open issue. Some further research is needed about handling traction discontinuities in a 3-D problem.

4. Numerical examples

The BRPIM is used for stress analysis of 2-D structures. Except when mentioned, the units are taken as standard international (SI) units in following examples.

4.1 Cantilever beam

The BRPIM is applied to obtain the solution of a cantilever beam, which is shown in Fig. 2. A plane stress problem is considered. The elastic constants for the beam are: $E = 3.0 \times 10^7$, and $\nu = 0.3$. The length L and height D of beam are 48 and 12, respectively. The beam is subjected to a parabolic traction at the free end. The analytical solution is available (see Timoshenko and Goodier 1970), for which

The stress components are given by

$$\sigma_x(x, y) = \frac{P(L-x)y}{I} \tag{17a}$$

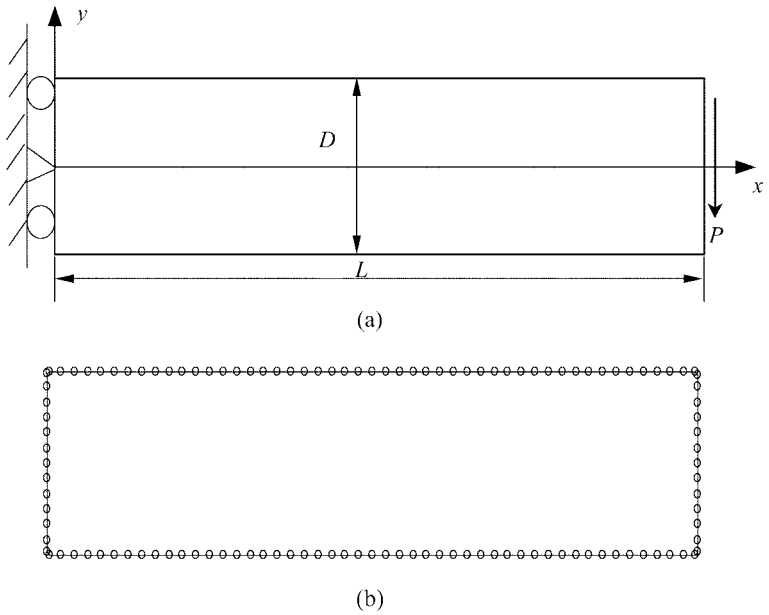

Fig. 2(a) A cantilever beam, (b) Nodal arrangement of the cantilever beam

$$\sigma_y(x, y) = 0 \tag{17b}$$

$$\tau_{xy}(x, y) = \frac{P}{2I}\left[\frac{D^2}{4} - y^2\right] \tag{17c}$$

where I is the moment of inertia.

Parameters on the performance of the present BRPIM are investigated firstly. In following parameter investigations, a total of 120 uniform boundary nodes are used to discretize the boundary of the beam. One hundred twenty uniform integration cells are used to evaluate the integrals. We define the following norm as an error indicator to reflect the accuracy for the shear stress, as the shear stress is much more critical than the other stress components

$$e_t = \frac{1}{N}\sqrt{\sum_{i=1}^{N} (\tau_i^{Num} - \tau_i^{Exact})^2 \Big/ \sum_{i=1}^{N} \tau_i^{Exact^2}} \tag{18}$$

where N is the number of nodes investigated, τ^{Num} is the shear stress obtained numerically, and τ^{Exact} is the analytical shear stress.

4.1.1 Effects of radial function parameters

The multi-quadrics (MQ) radial function (Eq. 3) is used as basis function in this paper. Two parameters, C and q, will influence the performance of MQ radial functions (Kansa 1990, Franke and Schaback 1997, Sharan *et al.* 1997). C is defined as

$$C = c_0 d_i \tag{19}$$

where, c_0 is a coefficient chosen. The d_i is the shortest distance between the node i and neighbor nodes.

The parameter, q, is firstly investigated. From Eq. (4), q is taken as –1.5, –0.5, 0.5, and 1.5. Shear stresses for different q are obtained and compared with the analytical solution. Errors for different q are plotted in Fig. 3(a). From this figure, it can be observed that $q = 0.5$ leads to a better result in the range of studies. Hence, 0.5 is used in following studies.

Errors in shear stresses of different c_0 are plotted in Fig. 3(b). From Fig. 3(b), we can find that $c_0 = 1.0$-6.0 leads a satisfied result. For convenience, $c_0 = 2.0$ will be used in following studies.

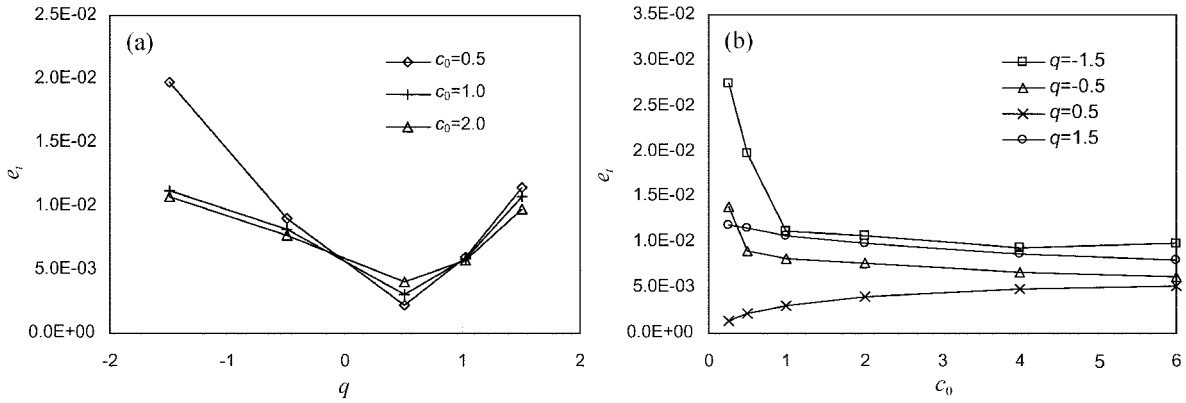

Fig. 3 Influence of parameters q and c_0 of MQ radial function (a) q, (b) c_0

4.1.2 Effects of interpolation domain

The size of influence domain of a quadrature point (sampling point) is decided by the parameter α_0 in Eq. (10). Results of $\alpha_0 = 1.0$~5.0 are obtained and plotted in Fig. 4. It can be found that results of $\alpha = 3.0$~4.5 (about 6~10 nodes used in a influence domain) are very good. An influence domain taken too small (α_0<2.5) and an influence domain taken too large ($\alpha_0 > 4.5$) lead to lager errors. The poor accuracy of a very small influence domain is due to the fact that there are not enough nodes to perform interpolation for the field variable. In the contrary, a very large influence

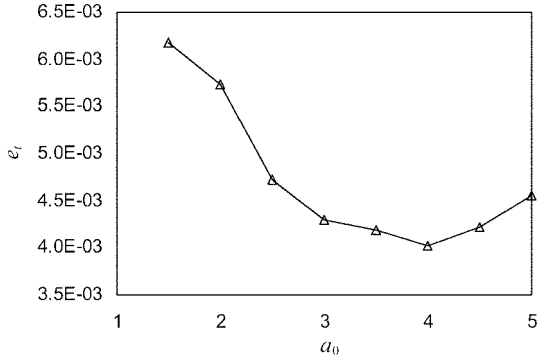

Fig. 4 Influence of the parameter α_0 of the interpolation domain

domain will increase the numerical error of interpolation because there are too many nodes to perform interpolation. Therefore, α_0 = 3.0~4.5 leads to acceptable results. For convenience and consistency, α_0 = 4.0 will be used in the following studies.

4.1.3 Results of the beam

Fig. 5 illustrates the comparison between the shear stress calculated analytically and by the one obtained by the BRPIM at the section of $x = L/2$. The plot shows a good agreement between the analytical and numerical results. The conventional linear BEM results of this problem are also shown in the same figure for comparison. The density of the nodes in BEM and the BRPIM is exactly the same. It is seen that the BRPIM results are more accurate than BEM results. This is because the BRPIM uses more nodes for the interpolation of the displacement and traction.

The convergence for the shear stresses at the section of $x = L/2$ with mesh refinement is shown in Fig. 6, where h is a characteristic length equivalent to the maximum element size in BEM. Three kinds of nodal arrangement of 72, 240 and 480 uniform boundary nodes are used. It is observed that the convergence of the BRPIM is very good. The convergences of BNM and the conventional linear BEM are also shown in the same figure. It is observed that BRPIM has a higher accuracy than BEM and BNM.

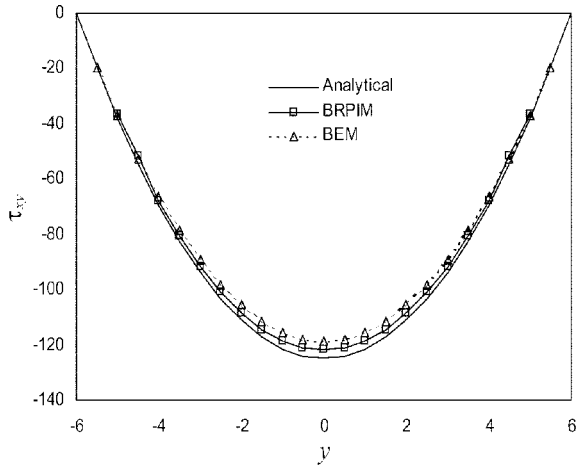

Fig. 5 Shear stress at the section $x = L/2$ of the beam

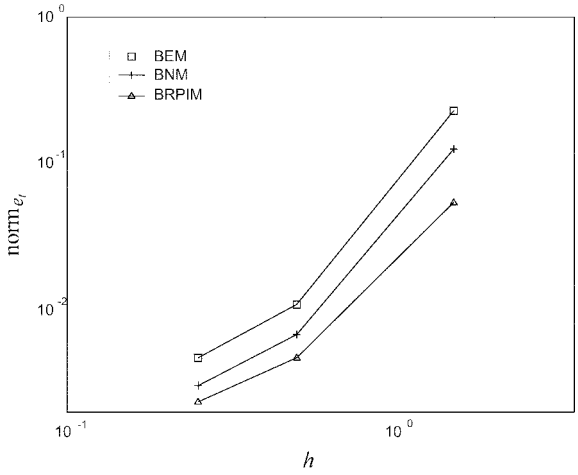

Fig. 6 Convergence in e_t norm of error

4.2 Internal pressurized hollow cylinder

A hollow cylinder under internal pressure is shown in Fig. 7. The parameters are taken as $p = 100$, $G = 8000$, and $\nu = 0.25$. This problem has been used by several other authors (Brebbia 1978) as a benchmark problem, as the analytical solution is available. Due to the symmetry of the problem, only one quarter of the cylinder (Fig. 8) needs to be modeled. The boundary of this domain is discretized by 30 nodes (6 uniformly distributed nodes on *ab*, *cd* and *ad*, and 12 uniformly distributed nodes on *bc*). The same number integration background cells are used. Three internal points A, B, and C are selected for examination. The polar coordinates for the three internal points are A(13.75, π/4), B(17.5, π/4) and C(21.25, π/4).

The BRPIM results are compared with the BNM, the conventional BEM and the analytical solution. The radial displacements of boundary nodes and internal points are presented in Table 2. The circumferential stresses σ_θ at points A, B and C are listed in the same table. It can be found that BRPIM results are in very good agreement with the analytical solution. In comparison with conventional BEM and BNM results, the BRPIM solution is, in general, more accurate for the both displacements and stresses.

4.3 Plate with a hole

A plate with a circular hole subjected to a unidirectional tensile load of 1.0 in the *x*-direction is considered. Due to symmetry, only the upper right quadrant (size 10 × 10) of the plate is modeled as

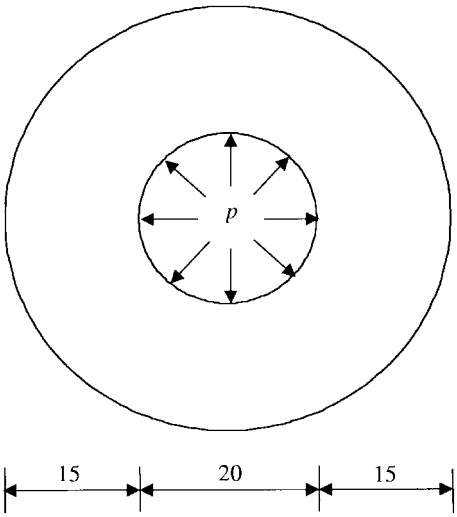

Fig. 7 Hollow cylinder subjected to internal pressure

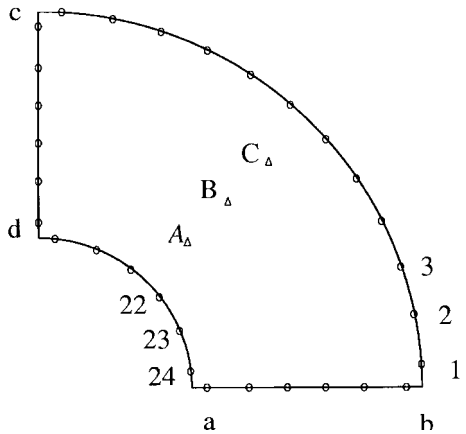

Fig. 8 Arrangement of nodes for the hollow cylinder

Table 2 Radial displacement and circumferential stresses for hollow cylinder

	Nodes	Exact.	BRPIM	BNM	BEM
Radial displacements ($\times 10^{-2}$)	1	0.4464	0.4466	0.4462	0.4468
	2	0.4464	0.4475	0.4463	0.4482
	3	0.4464	0.4493	0.4498	0.4494
	22	0.8036	0.8200	0.8220	0.8266
	23	0.8036	0.8207	0.8215	0.8268
	24	0.8036	0.8215	0.8223	0.8251
	A	0.6230	0.6211	0.6256	0.6319
	B	0.5294	0.5366	0.5353	0.5374
	C	0.4766	0.4810	0.4826	0.4838
Stress σ_θ	A	82.0113	82.1437	81.8513	82.0192
	B	57.9226	58.2585	58.1627	58.1691
	C	45.4112	45.6264	45.4597	45.6575

shown in Fig. 9. When the condition $b/a \geq 5$ is satisfied, the solution of finite plate is very close to that of the infinite plate (Roark 1975). Plane strain condition is assumed, and $E = 1.0 \times 10^3$, $\nu = 0.3$. Symmetry conditions are imposed on the left and bottom edges, and the inner boundary of the hole is traction free. The tensile load in the x direction is imposed on the right edge. The exact solution for the stresses of infinite plate is available (Timoshenko and Goodier 1970):

$$\sigma_x(x, y) = 1 - \frac{a^2}{r^2}\left(\frac{3}{2}\cos 2\theta + \cos 4\theta\right) + \frac{3a^4}{2r^4}\cos 4\theta \tag{20a}$$

$$\sigma_y(x, y) = -\frac{a^2}{r^2}\left(\frac{1}{2}\cos 2\theta - \cos 4\theta\right) - \frac{3a^4}{2r^4}\cos 4\theta \tag{20b}$$

$$\sigma_{xy}(x, y) = -\frac{a^2}{r^2}\left(\frac{1}{2}\sin 2\theta + \sin 4\theta\right) + \frac{3a^4}{2r^4}\sin 4\theta \tag{20c}$$

where (r, θ) are the polar coordinates with the origin at the centre of the hole, and θ is measured counter-clockwise from the positive x axis.

A total of 68 nodes are used to discretize the boundary (with 10 uniformly distributed nodes on BC, CD and AE, and 19 nonuniformly distributed nodes along AB and DE). The same number of integration background cells are used. As the stress is more critical in the assessment of solution accuracy, detailed results of stress are presented here. The stress σ_x at $x = 0$ obtained by the BRPIM is given in Fig. 10 together with the analytical solution for the infinite plate. BEM results of this problem are also shown in the same figure for comparison. It is observed from the figure that the BRPIM gives satisfactory results for this problem. It is clearly shown that the BRPIM possesses slightly higher accuracy than linear BEM for this problem.

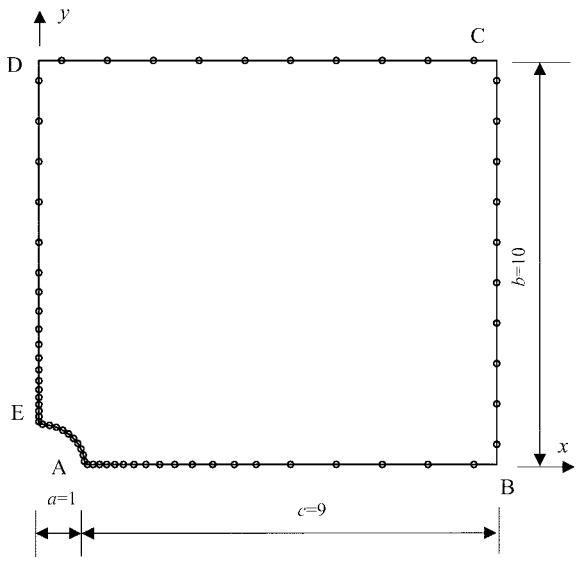

Fig. 9 Nodes in a plate with a central hole subjected to a unidirectional tensile load in the x direction

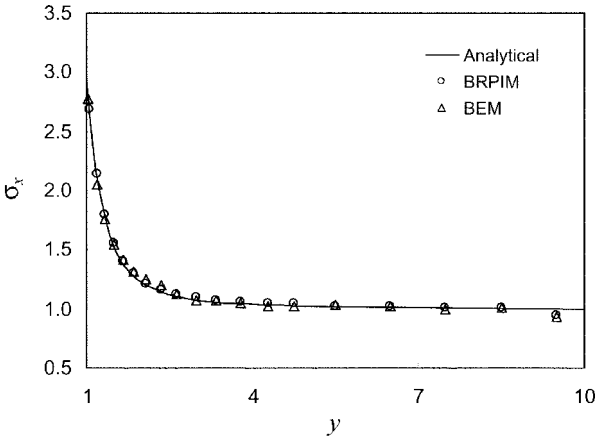

Fig. 10 Stress σ_x distribution in a plate with a central hole subjected to a unidirectional tensile load

5. Conclusions

A Boundary Radial Point Interpolation Method (BRPIM) for 2-D structural analyses has been presented in this paper. The boundary integral equation is discretized using radial basis point interpolation based on a group of arbitrarily distributed nodes on the boundary of problem domain. The BRPIM does not require any element connectivity in constructing the system equation, and possesses the dimensionality advantage. Numerical examples are presented for stress analysis of two-dimensional solids. Some important parameters on the performance of the present method are investigated in detail. From the studies in this paper, the following conclusion can be drawn:

1) Using radial function basis in the BRPIM, the interpolation is stable and flexible for arbitrary distributed nodes.
2) Compared with BEM, major advantages of the BRPIM are meshless and better accuracy. Major disadvantages of the BRPIM are complexity of algorithm, some undefined parameters, and more computational cost.
   Compared with BNM, major advantages of the BRPIM are that it is easier to satisfy boundary conditions and has better computational efficiency.
3) For MQ radial function, q = 0.5 and c_0 = 1.0-6.0 leads to acceptable results for most problems studied. q = 0.5 and c_0 = 2.0 are recommended
4) The size of influence domain of α_0 = 3.0~4.5 should be used for most problems studied.
5) Numerical examples are presented to demonstrate the convergence, validity and efficiency of the present method. The results presented are indeed very encouraging. It is demonstrated that the BRPIM is easy to implement (the implementation of the BRPIM is as easy as that of the conventional BEM), and very flexible for solving 2-D structural analyses.

In this paper, the BRPIM is used to solve 2-D elastic problems. In the BRPIM, the radial basis point interpolation is used. There is no difficulty to extend the presented radial basis point interpolation to 3-D problems because the variable in RBF is only the distance. In addition, it has been proven that the existence and efficiency of the radial basis point interpolation for arbitrary scattered nodes. Hence, the BRPIM can be extended to solve 3-D problems to take the full advantages of the meshfree concept. However, because of the complexity of 3-D problems, a lot of research work is required.

References

Atluri, S.N. and Zhu, T. (1998). "A new meshless local Petrov-Galerkin (MLPG) approach in computational mechanics", *Comput. Mech.*, **22**, 117-127.

Belytschko, T., Lu, Y.Y. and Gu, L. (1994). "Element-Free Galerkin methods", *Int. J. Numer. Methods Engrg.*, **37**, 229-256.

Belytschko, T. and Organ, D. (1995). "Coupled finite element-element-free Galerkin method", *Comput. Mech.*, **17**, 186-195.

Brebbia, C.A. (1978). *The Boundary Element Method for Engineers.* Pentech Press, London, Halstead Press, New York.

Brebbia, C.A., Telles, J.C. and Wrobel, L.C. (1984). *Boundary Element Techniques.* Springer Verlag, Berlin.

Chati, M.K., Mukherjee, S. and Mukherjee, Y.X. (1999). "The boundary node method for three-dimensional linear elasticity", *Int. J. Numer. Methods Engrg.*, **46**, 1163-1184.

Chati, M.K. and Mukherjee, S. (2000). "The boundary node method for three-dimensional problems in potential theory", *Int. J. Numer. Methods Engrg.*, **47**, 1523-1547.

De, S. and Bathe, K.J. (2000). "The method of finite spheres", *Comput. Mech.*, **25**, 329-345.

Franke, C. and Schaback, R. (1997). "Solving partial differential equations by collocation using radial basis functions", *Appl. Math. Comput.*, **93**, 73-82.

Gu, Y.T. and Liu, G.R. (2001). "A coupled Element Free Galerkin/Boundary Element method for stress analysis of two-dimension solid", *Comput. Methods Appl. Mech. Engrg.*, **190**, 4405-4419.

Hegen, D. (1996). "Element-free Galerkin methods in combination with finite element approaches", *Comput. Methods Appl. Mech. Engrg.*, **135**, 143-166.

Kansa, E.J. (1990). "Multiquadrics-a scattered data approximation scheme with applications to computational fluid dynamics", *Computers Math. Applic.*, **19**(8/9), 127-145.

Kothnur, V.S., Mukherjee, S. and Mukherjee, Y.X. (1999). "Two-dimensional linear elasticity by the boundary node method", *Int. J. Solids Struct.*, **36**, 1129-1147.

Liu, G.R. (2002), *Mesh Free Methods: Moving Beyond the Finite Element Method*. CRC press, Boca Raton, USA.

Liu, G.R. and Gu, Y.T. (2000). "Coupling element free Galerkin and hybrid boundary element methods using modified variational formulation", *Comput. Mech.*, **26**, 166-173.

Liu, G.R. and Gu, Y.T. (2001a). "A point interpolation method for two-dimensional solid", *Int. J. Numer. Methods Engrg.*, **50**, 937-951.

Liu, G.R. and Gu, Y.T. (2001b). "A local point interpolation method for stress analysis of two-dimensional solids", *Struct. Eng. Mech.*, **11**(2), 221-236.

Liu, G.R. and Gu, Y.T. (2001c), "A Local Radial Point Interpolation Method (LRPIM) for free vibration analyses of 2-D solids", *J. Sound Vib.*, **246**(1), 29-46.

Liu, G.R., Yan, L., Wang, J.G. and Gu, Y.T. (2002). "Point interpolation method based on local residual formulation using radial basis functions", *Struct. Eng. Mech.*, **14**(6), 713-732.

Mukherjee, Y.X. and Mukherjee, S. (1997). "Boundary node method for potential problems", *Int. J. Numer. Methods Engrg.*, **40**, 797-815.

Nayroles, B., Touzot, G. and Villon, P. (1992). "Generalizing the finite element method: diffuse approximation and diffuse elements", *Comput. Mech.*, **10**, 307-318.

Roark, R.J. and Young, W.C. (1975). *Formulas for Stress and Strain.* McGraw-hill, London.

Sharan, M., Kansa, E.J. and Gupta, S. (1997). "Application of the multiquadric method for numerical solution of elliptic partial differential equations", *Applied Mathematics and Computation*, **84**, 275-302.

Wang, J.G. and Liu, G.R. (2002), "On the optimal shape parameters of radial basis functions used for 2-D meshlesss methods", *Comput. Methods Appl. Mech. Eng.*, **191**, 2611-2630.

Timoshenko, S.P. and Goodier, J.N. (1970). *Theory of Elasticity.* 3rd Edition. McGraw-hill, New York.